Improved Method for the Lateral Vibration Analysis of a Rotor System

Eric K. L. Yee* and Y. G. Tsuei†
University of Cincinnati, Cincinnati, Ohio 45221-0072

A component modal synthesis technique for calculating the system dynamics of a rotor system is presented. In this method, the rotor system is divided into bladed disks, rotor shafts, and the nonrotating subsystems. The subsystem frequency transfer function matrices, geometric compatibility, and force equilibrium equations are combined to solve the critical speeds of the rotor system. The degrees of freedom in the final critical speed equation are reduced to the number of physical connections between subsystems. It is much smaller than the total number of substructure modes used in the synthesis. The proposed technique is capable of handling the rotor system with frequency-dependent properties, such as bearing stiffness. The method applies equally well for the synchronous and nonsynchronous rotor whirl. Numerical results indicate that the proposed method can efficiently and accurately determine the dynamic characteristics of a rotor system.

Nomenclature

$\bar{f}$ = modal force vector $\bar{H}\bar{f}=0$
$f, f(t)$ = force vector in frequency domain and time domain, respectively
f_{IJ} = interconnecting force vector at the junction between substructures I and J
$f_{KI,y}$ = force in y direction acting on the Kth bladed disk from the Ith rotor shaft
$f_{KI,\theta}$ = moment in θ direction acting on the Kth bladed disk from the Ith rotor shaft
$H_{ij}^{I}(\omega)$ = frequency transfer matrix of substructure I at row i, column j
$\bar{H}(\omega)$ = modal force matrix from $\bar{H}\bar{f}=0$
I_{dK} = mass transverse moment of inertia of the Kth bladed disk
I_{pK} = mass polar moment of inertia of the Kth bladed disk
I_p ratio = ratio of polar moment of inertia to the baseline polar moment of inertia ($I_p/I_{p-\text{baseline}}$)
K = stiffness matrix
k_r = rth modal stiffness
M = mass matrix
m_r = rth modal mass
$p(t)$ = modal coordinate vector
$x, x(t)$ = response vector in frequency domain and time domain, respectively
x^I = response vector of substructure I
x_{IJ} = response vector at the junction between substructures I and J
Λ = diagonal matrix of eigenvalues
λ_r = rth eigenvalue of a structure
μ_I = whirl ratio, Ith rotor-shaft whirl frequency to the vibratory frequency
Φ = modal matrix
ϕ_r = rth eigenvector or modal vector
ω = angular frequency of excitation
ω_r = rth natural frequency of a structure

Superscript
I = substructure I

Introduction

DYNAMIC analysis of the rotor system is quite different from the analysis of the nonrotating structures. The rotor analysis can be mainly divided into three different categories: lateral, axial, and torsional analyses. Within these three types of analyses, the lateral analysis is the most widely used and is of primary interest. This paper concentrates on an improved substructure modal synthesis technique for the lateral vibration of a rotor system.

For the lateral critical speed analysis, the gyroscopic effects due to the whirling motion of the rotor shaft are significant and have to be included for analysis. The gyroscopic moments from the forward rotor whirl motion tend to stiffen the rotor shaft, thereby increasing the critical speeds. On the other hand, the gyroscopic effects from the backward rotor whirl motion soften the rotor shaft and decrease the critical speeds. It is because of these gyroscopic effects that the critical speeds of a rotor system, unlike the nonrotating structure, depend not only on the system configuration but also on the direction and frequency of the rotor whirl motion. To further complicate the analysis, some system component properties, such as the squeeze film damper bearing, are also frequency dependent.

The dynamic characteristics of a structure can be obtained by component mode synthesis techniques. Hurty[1] introduced the fixed-boundary normal mode method where the substructure modes were divided into three types: rigid-body modes, normal modes, and constraint modes. The constraint mode is determined by applying a unit displacement to one of the redundant constraints, while keeping the other constraints fixed. Hale and Meirovitch[2] used the admissible shape vectors and subspace iteration technique to obtain the eigensolution of the system. Craig and Bampton[3] simplified the procedure of Hurty's method,[1] and the rigid-body modes were included in the constraint mode category. Hou[4] presented a synthesis method using the free-free substructure modes and also discussed an error analysis procedure. The approximation and transformation techniques were also incorporated by Benfield and Hruda,[5] Rubin,[6] Hintz[7] for improving the solution accuracy and computation efficiency.

Received June 23, 1988; revision received March 23, 1989.

*Graduate Student, Structural Dynamics Research Laboratory, Department of Mechanical and Industrial Engineering; currently Mechanical Engineer, Systems Engineering and Standardization Department, Naval Air Engineering Center, Lakehurst, NJ.

†Professor, Structural Dynamics Research Laboratory, Department of Mechanical and Industrial Engineering. Member AIAA.

Gunter et al.[8] discussed a procedure for calculating the damped eigenvalues of a rotor system. The constraint normal modes and rigid-body modes of the rotor components were used in this method. Rajan et al.[9] presented a method for calculating the critical speed sensitivities with respect to different rotor parameters. Childs[10] discussed a modal simulation model for a rotor. Li and Gunter[11,12] derived a component mode synthesis method for determining the dynamics of a rotor system. They also studied the truncation errors when an incomplete component modal set was used to compute the rotor dynamics. Adams and Padovan[13,14] decomposed the bearing stiffness and damping matrices of a rotor system into symmetric and skew symmetric matrices. They also discussed an approach for including the rotor-stator interactive forces in a linearized rotor-bearing model. Nelson and Meacham[15] applied the component mode synthesis method to calculate the transient response of a rotor system.

A different approach is suggested here, and this method is an extension of the component mode synthesis method, modal force method, discussed by Yee and Tsuei.[16] The method has the capability of including the frequency-dependent properties for analysis. It is because of this additional capability that the method is well suited for the lateral vibration analysis of a rotor system. In this method, the frequency transfer function matrix of each subsystem is obtained from either experimental testing or finite-element modal analysis. The subsystem modes to be included in the analysis for formulating the frequency transfer function matrix depend on the solution frequency ranges, the nature of the rotor systems, and the accuracy of the solution desired. The inertia restraint from the low-frequency modes and the residual flexibility of the high-frequency modes as discussed by MacNeal[17] and Klosterman[18] can be used to improve the accuracy of the solution. The types of substructure modes used in the analysis can be constraint modes as discussed by Hurty[1] or the attachment modes suggested by Bamford.[19] In other words, the frequency transfer function matrix of each substructure can be represented by any type of substructure mode or its approximation, such as rigid-body modes, normal modes, constraint modes, and attachment modes, as long as the frequency transfer function matrix of each subsystem is accurately represented in the frequency range of interest.

The frequency transfer function matrix of each substructure is further partitioned into two sets. One set is the internal degrees of freedom, and the other set is the boundary degrees of freedom. The internal degrees of freedom do not connect to other substructures, and the boundary degrees of freedom are connected to the other substructures.

The concept of this method is to transform the substructure physical degrees of freedom to substructure modal coordinates, select a truncated substructure modal set to formulate the subsystem frequency transfer function matrix, and then further reduce that matrix to the number of physical boundary degrees of freedom by the partitioning process. The boundary coordinate frequency transfer function matrices of substructures become the basic building blocks for synthesizing the final system critical speed equation. The order of the system critical speed equation is equal to the number of physical boundary coordinates between subsystems and is frequency dependent. The number of physical boundary degrees of freedom is usually smaller than the number of substructure modes used and is the subset of physical degrees of freedom of the entire rotor system.

Derivation of the Subsystem Frequency Transfer Function Matrix

Classification of the Rotor Subsystems

The rotor system, as shown in Fig. 1, can be divided into three main subsystems. The first type is the bladed-disk subsystem, which rotates, and the gyroscopic effects must be included for system critical speed analysis. The second type is the rotor shaft subsystem, which also rotates, but the gyroscopic effects of this subsystem are small and can be neglected. The third type is the nonrotating subsystem. The rotor casing and its support structures belong to this category.

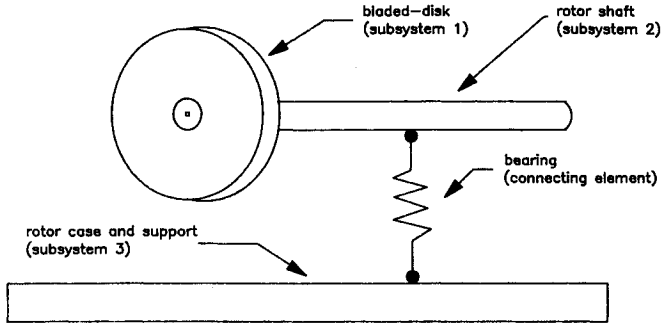

Fig. 1 Simplified rotor system.

Modal Analysis of the Rotor-Shaft Subsystem

The gyroscopic effects of the rotor-shaft subsystem (with the bladed disks detached) can be neglected during the critical speed analysis because of its relatively small magnitude when it is compared to the bending stiffness of the shaft. With this approximation, the vibration characteristics of the rotor-shaft subsystem can be calculated by modal analysis, which is presented later in the paper.

The equation of motion for a substructure without damping is represented by

$$M\ddot{x}(t)+Kx(t)=f(t) \tag{1}$$

The natural frequencies and mode shapes of the substructure can be obtained by solving the homogeneous differential equation

$$M\ddot{x}(t)+Kx(t)=0 \tag{2}$$

Let λ_r and ϕ_r be the rth mode eigenvalue and eigenvector; hence, the following orthogonality properties

$$\Phi^T M\Phi = I$$

$$\Phi^T K\Phi = \Lambda$$

are obtained, where the Φ is defined by

$$\Phi = [\phi_1 \quad \phi_2 \quad \ldots \quad \phi_N]$$

Since Φ is the modal matrix obtained by solving Eq. (2), $x(t)$ can be represented by

$$x(t)=\Phi p(t)$$

By using the preceding transformation, Eq. (1) becomes

$$M\Phi\ddot{p}(t)+K\Phi p(t)=f(t)$$

For harmonic excitation at ω, which is different from the ω_r, the response function can be expressed as

$$x(t)=\Phi[\Lambda-\omega^2 I]^{-1}\,\Phi^T f(t) \tag{3a}$$

or

$$x=H(\omega)f \tag{3b}$$

where $f(t)=f\,e^{i\omega t}$ and $x(t)=x\,e^{i\omega t}$ are used. It is noted that x is a function of frequency. Since $[\Lambda-\omega^2 I]$ is a diagonal ma-

trix, the transfer matrix

$$H(\omega)=\Phi\ [\Lambda-\omega^2 I]^{-1}\ \Phi^T$$

can be obtained by simple multiplication when the eigensolution of the substructures Φ are provided.

The complete modal set of substructure is not needed for calculating the frequency transfer function in Eq. (3). Only the modes in the neighborhood of the interested frequency ranges are to be included for analysis. The inertia restraint of low-frequency modes and residual flexibility of high-frequency modes can also be included into Eq. (3) for improving the accuracy of the frequency transfer function matrices. Equation (3) is further transformed as follows:

$$x=\sum_{r=1}^{L-1}\frac{(-\phi_r^T f)\phi_r}{\omega^2 m_r}+\sum_{r=L}^{h}\frac{(-\phi_r^T f)\phi_r}{m_r[\omega^2-\omega_r^2]}+\sum_{r=h+1}^{N}\frac{(\phi_r^T f)\phi_r}{k_r}$$

where

$$\sum_{r=1}^{L-1}\frac{(-\phi_r^T f)\phi_r}{\omega^2 m_r}$$

is the inertia restraint of low-frequency modes, and

$$\sum_{r=h+1}^{n}\frac{(\phi_r^T f)\phi_r}{k_r}$$

is the residual flexibility of high-frequency modes.

The types of modes included in Eq. (3) can be constraint modes, attachment modes, or the inertia relief modes, as long as the transfer matrix in the interested frequency ranges is accurately represented.

Partition of Frequency Transfer Function Matrix

Equation (3) can be partitioned as

$$\begin{bmatrix} x_{II} \\ x_{IJ} \\ \cdots \\ \cdots \\ \cdots \\ x_{IK} \end{bmatrix} = \begin{bmatrix} H_{II}^I(\omega) & H_{IJ}^I(\omega) & \cdots & H_{IK}^I(\omega) \\ H_{JI}^I(\omega) & H_{JJ}^I(\omega) & \cdots & H_{JK}^I(\omega) \\ \cdots & \cdots & \cdots & \cdots \\ \cdots & \cdots & \cdots & \cdots \\ \cdots & \cdots & \cdots & \cdots \\ H_{KI}^I(\omega) & H_{KJ}^I(\omega) & \cdots & H_{KK}^I(\omega) \end{bmatrix} \begin{bmatrix} f_{II} \\ f_{IJ} \\ \cdots \\ \cdots \\ \cdots \\ f_{IK} \end{bmatrix} \tag{4}$$

The graphic interpretation of the connecting terminology is shown in Fig. 2.

The purpose of such a partition, which will be demonstrated in later sections, is to facilitate the components coupling process and to reduce the system coordinates to the joint coordinates between substructures.

Nonrotating Subsystem

The frequency transfer function matrices of the nonrotating subsystems, such as rotor case, pylon, and cowling, can be derived using the same procedure as discussed in the rotor-shaft subsystem.

Bladed-Disk Subsystem

The equation of motion for the bladed-disk subsystem is different from the rotor-shaft and nonrotating subsystems. The gyroscopic effects, resulting from the whirling motion of the rotor-shaft assembly, must be included in the analysis. For most lateral analyses of the rotor system dynamics, each bladed disk can be treated as a rigid rotating disk. As a result of this assumption, the frequency transfer function equation

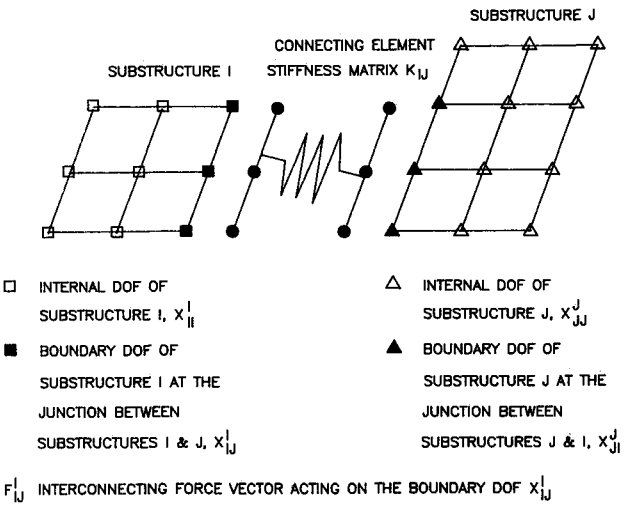

Fig. 2 Illustration of connecting terminology.

of each rotating bladed disk can be approximated as

$$\begin{bmatrix} y_{KI} \\ \theta_{KI} \end{bmatrix} = \begin{bmatrix} \dfrac{-1}{m_K\omega^2\mu_I^2} & 0 \\ 0 & \dfrac{1}{(I_{pK}+I_{dK}\mu_I)\omega^2\mu_I} \end{bmatrix} \begin{bmatrix} f_{KI,y} \\ f_{KI,\theta} \end{bmatrix} \tag{5}$$

where m_K is the mass of the Kth bladed disk.

Equation (5) can be rewritten into generic form as

$$x_{KI}=H_{II}^K(\omega)f_{KI} \tag{6}$$

The subscript KI of Eq. (6) indicates that the Kth bladed disk is attached to the Ith rotor-shaft subsystem.

Synthesization of the Rotor System

Subsystem Frequency Transfer Function Matrix

The procedures of coupling the subsystems into the final rotor system will be demonstrated on a simple rotor system as shown in Fig. 1.

From Eq. (4), the frequency transfer function equation of the bladed disk, subsystem 1 is

$$x^1=x_{12}=H_{11}^1(\omega)f_{12} \tag{7a}$$

For the rotor shaft, subsystem 2 is

$$x^2=\begin{bmatrix} x_{21} \\ x_{22} \\ x_{23} \end{bmatrix}=\begin{bmatrix} H_{11}^2(\omega) & H_{12}^2(\omega) & H_{13}^2(\omega) \\ H_{21}^2(\omega) & H_{22}^2(\omega) & H_{23}^2(\omega) \\ H_{31}^2(\omega) & H_{32}^2(\omega) & H_{33}^2(\omega) \end{bmatrix}\begin{bmatrix} f_{21} \\ f_{22} \\ f_{23} \end{bmatrix} \tag{7b}$$

For the rotor case, subsystem 3 is

$$x^3=\begin{bmatrix} x_{32} \\ x_{33} \end{bmatrix}=\begin{bmatrix} H_{11}^3(\omega) & H_{12}^3(\omega) \\ H_{21}^3(\omega) & H_{22}^3(\omega) \end{bmatrix}\begin{bmatrix} f_{32} \\ f_{33} \end{bmatrix} \tag{7c}$$

The external force vectors are zero vectors for the critical speed analysis. The following equations are obtained:

$$f_{22}=0 \tag{8a}$$

$$f_{33}=0 \tag{8b}$$

Geometric Compatibility and Force Equilibrium Equations

The conditions for geometric compatibility and force equilibrium are expressed as

$$K_{11}^4(x_{32}^3 - x_{23}^2) = f_{23} \quad \text{or} \quad x_{32}^3 - x_{23}^2 = H_{11}^4 f_{23} \tag{9a}$$

$$x_{12}^1 = x_{21}^2 \tag{9b}$$

$$f_{23} = -f_{32} \tag{9c}$$

$$f_{21} = -f_{12} \tag{9d}$$

where the K_{11}^4 and H_{11}^4 are the connecting bearing stiffness and flexibility matrices, respectively, between the rotor-shaft and rotor-case subsystems.

Coupling the Bladed-Disk, Rotor-Shaft, and Rotor-Case Components

The final rotor system can be synthesized by coupling the bladed disk, rotor shaft, and rotor case together. Equations (7-9) are combined and simplified. The following equation is derived:

$$\begin{bmatrix} H_{22}^1(\omega) + H_{11}^2(\omega) & -H_{13}^2(\omega) \\ -H_{31}^2(\omega) & H_{33}^2(\omega) + H_{11}^3(\omega) + H_{11}^4(\omega) \end{bmatrix} \begin{bmatrix} f_{12} \\ f_{23} \end{bmatrix} = \begin{bmatrix} 0 \\ 0 \end{bmatrix} \tag{10a}$$

or

$$\bar{H}\bar{f} = 0 \tag{10b}$$

The critical speeds of the rotor system are determined by solving the characteristic equation, which is obtained by setting the determinant of the $\bar{H}(\omega)$ equal to zero:

$$\det \begin{vmatrix} H_{22}^1(\omega) + H_{11}^2(\omega) & -H_{13}^2(\omega) \\ -H_{31}^2(\omega) & H_{33}^2(\omega) + H_{11}^3(\omega) + H_{11}^4(\omega) \end{vmatrix} = 0$$

After the critical speed ω_r is calculated from Eq. (11), the eigenvector $\bar{f}$ for the rth mode can be obtained from the modal force Eq. (10).

Mode Shape

The rth mode system eigenvector x is recovered by substituting the corresponding modal force vector $\bar{f}_r$ back into Eq. (7).

Numerical Results and Examples

A rotor system was analyzed using the proposed method. The system components are shown in Fig. 3, and the synthesized rotor system configuration is shown in Fig. 4. The system has three bladed disks, a rotor shaft, and a rotor case. The bladed disks are connected to the rotor shaft at the node 1, 3, and 5 locations. Two bearings are used to join the rotor shaft and the rotor casing. Node 2 is connected to node 6 by bearing 1, and node 4 is connected to node 7 by bearing 2. The material properties and geometric dimensions of the system components are tabulated in Table 1. Ten rotor-shaft modes (2 rigid-body modes and 8 flexible modes) and 8 rotor case modes (2 rigid-body modes, 4 prismatic modes, and 2 nonprismatic modes) were also included for analysis.

The critical speeds of the rotor system were determined from the normalized determinant curve, which is partially shown in Fig. 5. The first three critical speeds were found to be 219.9, 274.2, and 379.6 rad/s. The uniform normalization algorithm was used to calculate the system determinant. Some normalized determinants are relatively smaller than the other determinants, especially in the regions around the subsystem

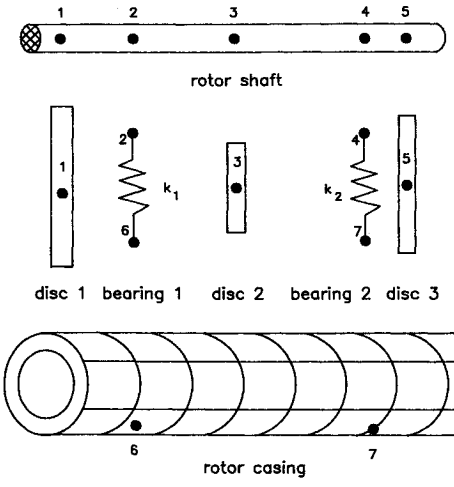

Fig. 3 Components of a rotor system.

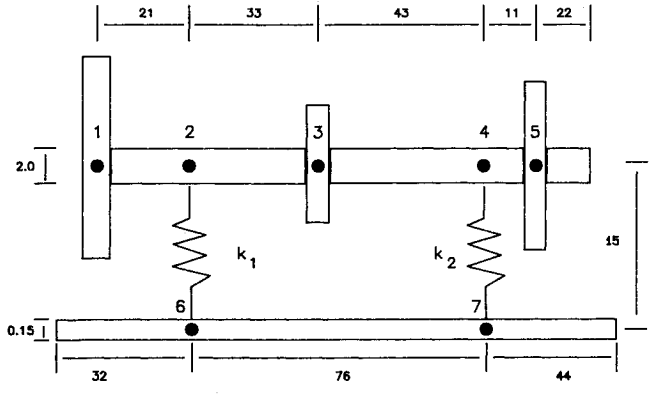

Fig. 4 Synthesized rotor system.

Table 1 Description of geometric and material properties of the rotor components

Bladed disk	Mass, g	I_p, g-cm^2	I_d, g-cm^2
Disk 1	2039.63	446,760	223,380
Disk 2	1073.49	235,140	117,570
Disk 3	1610.23	352,700	176,350

Bearing stiffness	K_{yy}, N/m	$K_{y\theta}$, N/rad	$K_{\theta y}$, Nm/m	$K_{\theta\theta}$, Nm/rad
Number 1	2.0×10^7	0.0	0.0	3000
Number 2	4.0×10^7	0.0	0.0	5000

Rotor shaft (round shaft)	
Length	130.00 cm
Radius	1.00 cm
Rotor casing (thin-wall cylinder)	
Length	152.00 cm
Mean radius	15.00 cm
Wall thickness	0.15 cm
Material properties (steel)	
Density	7.80 g/cm^3
Modulus of elasticity	1.96×10^7N/cm^3
Poisson's ratio	0.30

natural frequencies. However, the frequencies where small determinants were calculated are not necessarily the system critical speeds. The system critical speeds occur only at the change sign of the normalized determinant. After the critical speeds were found, the mode shapes of the rotor shaft were calculated from Eq. (7) and are plotted in Fig. 6.

The effects of the bladed-disk gyroscopic moments due to a forward synchronous rotor whirl on the system critical

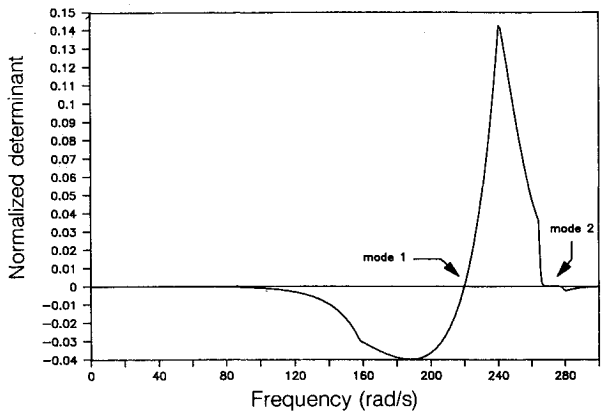

Fig. 5 Normalized determinant curve of the rotor system; synchronous rotor whirl.

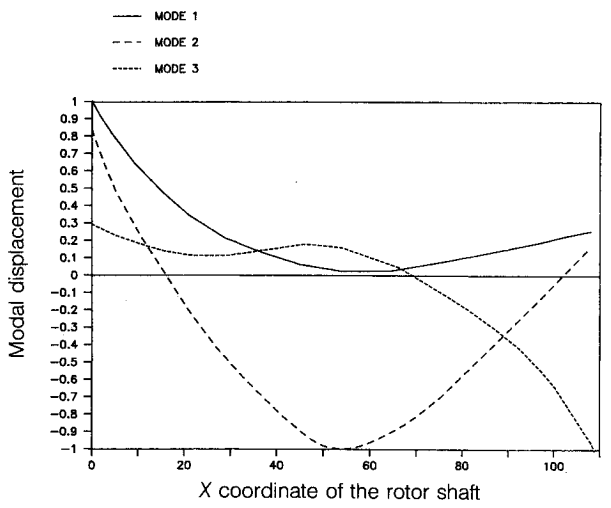

Fig. 6 Mode shapes of the rotor system; synchronous rotor whirl.

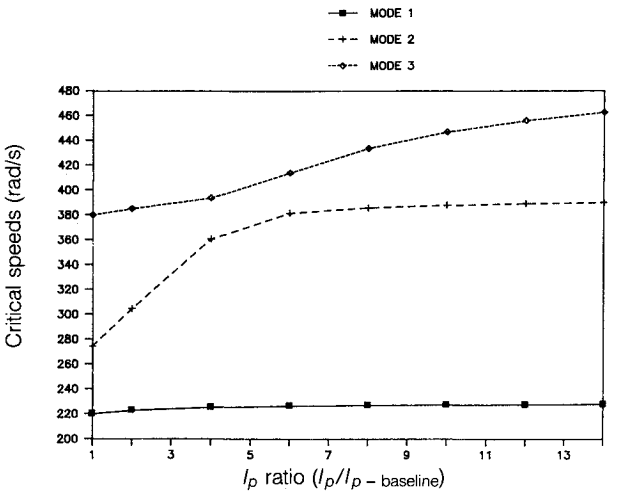

Fig. 7 Critical speeds of the rotor system vs the I_p ratio ($I_p/I_{p-\text{baseline}}$); synchronous rotor whirl.

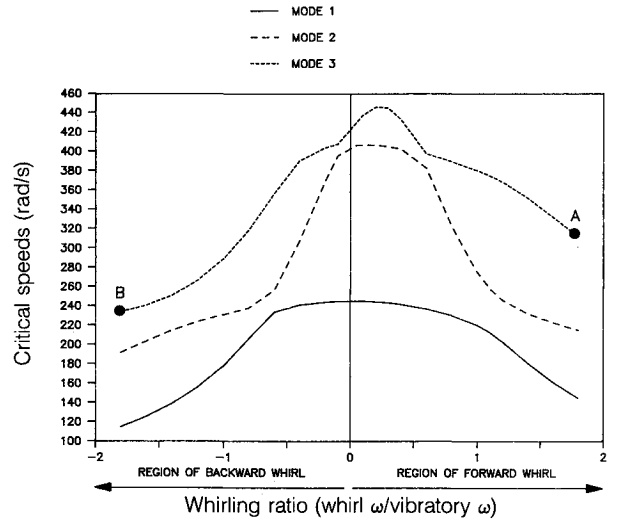

Fig. 8 Critical speeds of the rotor system vs the whirl ratio (whirl ω/vibratory ω); nonsynchronous rotor whirl.

speeds were studied, and the results are plotted in Fig. 7. The I_p ratio ($I_p/I_{p-\text{baseline}}$) can be used as an indicator for the change of the system gyroscopic moments. Consistent with known theoretical and experimental trends, as shown in Fig. 7, the rotor critical speeds increase with increased gyroscopic moments due to stiffening of the shaft. The stiffening effect is more pronounced on the second mode compared to the first and third modes. The second mode is the primary bending mode as shown in Fig. 6.

The critical speeds for the nonsynchronous forward and backward rotor whirl were also studied. Figure 8 shows that the first three critical speeds peak around zero whirling ratio (whirl ω/vibratory ω). The results can be explained as follows: As the whirling ratio approaches zero, both the mass and the rotational inertia of the bladed disks become zero. This is equivalent to the removal of the bladed disks from the system. Thus, the elimination of the bladed disks from the rotor system reduces the modal masses and the gyroscopic stiffening effect. The optimum whirling ratio necessary for this rotor system to have the maximum critical speeds is around 0.2, as depicted in Fig. 8.

As shown in Fig. 8, the third critical speeds at a whirl ratio of 1.8 (forward rotor whirl) is 311.5 rad/s (point A), and at a whirl ratio of -1.8 (backward rotor whirl) it is 233.6 rad/s (point B). The difference of the third critical speeds between the forward and backward rotor whirl configurations is 77.9 rad/s. Similar phenomena exist at the first and second critical speeds. It can be concluded that, with the same magnitude of whirling ratio, the critical speeds of the forward whirl rotor system are higher than the backward whirl rotor system. The results verify the fact that the gyroscopic moments from forward rotor whirl stiffen the rotor, and those from the backward rotor whirl soften it.

Conclusions

A component modal synthesis technique for analyzing the lateral dynamic characteristics of a rotor system is presented. This method divides a rotor system into three different categories of subsystems. The bladed-disk subsystem is a rotating component of the rotor system and has gyroscopic effects. The rotor-shaft subsystem is also a rotating component, but the gyroscopic effects can be neglected. The nonrotating subsystem includes all of the nonrotating structures, such as rotor casing and support. The rotor whirling frequency and the properties of coupling elements between subsystems, such as bearing stiffness, can also be defined as functions of vibratory frequency. This additional capability makes the suggested method very suitable for the dynamic analysis of the rotor systems. The advantages of this method are summarized as follows.

1) The order of the critical speed matrix equation is condensed to the number of physical connections between substructures and is much smaller than the total number of component modal coordinates or the physical coordinates of the entire rotor system.

2) The rotor whirling frequency and the system component properties can be defined as the functions of vibratory frequency, and because of that, the rotor system configuration

can be better represented. The synchronous and nonsynchronous rotor whirls of a rotor system can be analyzed efficiently.

3) Critical speeds in any frequency range can be calculated independently without prior calculation of lower or higher critical speed modes. This is particularly useful when only the solution within a frequency range is desired.

4) Force vectors acting on the system components are calculated during the solution process. They can be used later for dynamic stress calculations.

5) Experimental test data and the analytical data from the finite-element analysis of the system components can be included and merged for the final rotor system dynamics analysis without much difficulty.

6) The modal characteristics of the subsystems can be stored in the computer, and a new rotor configuration can be formed readily.

References

[1]Hurty, W. C., "Dynamic Analysis of Structural Systems Using Component Modes," *AIAA Journal*, Vol. 3, April 1965, pp. 678-685.

[2]Hale, A. L. and Meirovitch, L., "A Procedure for Improving Discrete Substructure Representation in Dynamic Synthesis," *AIAA Journal*, Vol. 20, Auig. 1982, pp. 1128-1136.

[3]Craig, R. and Bampton, M., "Coupling of Structures for Dynamic Analysis," *AIAA Journal*, July 1968, pp. 1313-1319.

[4]Hou, S. N., "Review of Modal Synthesis Techniques and a New Approach," *Shock and Vibration Bulletin*, Vol. 40, Pt. 4, Dec. 1969, pp. 25-30.

[5]Benfield, W. A. and Hruda, R. F., "Vibration Analysis of Structure by Component Mode Substitution," *AIAA Journal*, Vol. 9, July 1971, pp. 1255-1261.

[6]Rubin, S., "Improved Component Mode Representation," *AIAA Journal*, Vol. 13, Aug. 1975, pp. 995-1006.

[7]Hintz, R. M., "Analytical Methods in Component Modal Synthesis," *AIAA Journal*, Vol. 13, Aug. 1975, pp. 1007-1016.

[8]Gunter, E. J., Humphris, R. R., and Springer, H., "A Rapid Approach for Calculating the Damped Eigenvalues of a Gas Turbine on a Minicomputer: Theory," *Journal of Vibration, Acoustics, Stress and Reliability in Design*, Vol. 106, April 1984, pp. 239-250.

[9]Rajan, M., Nelson, H. D., and Chen, W. J., "Parameter Sensitivity in Dynamics of Rotor-Bearing Systems," *Journal of Vibration, Acoustics, Stress and Reliability in Design*, Vol. 108, April 1986, pp. 197-206.

[10]Childs, D. W., "A Rotor-Fixed Modal Simulation Model for Flexible Rotating Equipment," *Journal of Engineering for Industry*, Vol. 96, No. 2, May 1974, pp. 659-669.

[11]Li, D. F. and Gunter, E. J., "A Study of the Modal Truncation Error in the Component Mode Analysis of a Dual-Rotor System," *Journal of Engineering for Power*, Vol. 104, July 1982, pp. 525-532.

[12]Gunter, E. J. and Li, D. F., "Component Mode Synthesis of Large Rotor System," *Journal of Engineering of Power*, Vol. 104, July 1982, pp. 552-560.

[13]Adams, M. L. and Padovan, J., "Insights into Linearized Rotor Dynamics," *Journal of Sound and Vibration*, Vol. 76, No. 1, 1981, pp. 129-142.

[14]Adams, M. L., "Insights into Linearized Rotor Dynamics," *Journal of Sound and Vibration*, Vol. 112, No. 1, 1987, pp. 97-110.

[15]Nelson, H. D. and Meacham, W. L., "Transient Analysis of Rotor Bearing System Using Component Mode Synthesis," American Society of Mechanical Engineers, Paper 81-GT-110, March 1981.

[16]Yee, E. K. and Tsuei, Y. G., "A Direct Component Modal Synthesis Technique for System Dynamic Analysis," *AIAA Journal*, Vol. 27, No. 8, 1989, pp. 1083-1088.

[17]MacNeal, R. H., "A Hybrid Method of Component Mode Synthesis," *Computers and Structures*, Vol. 1, 1971, pp. 581-601.

[18]Klosterman, A. L., "A Combined Experimental and Analytical Procedure for Improving Automotive System Dynamics," Society of Automotive Engineers Paper 720093, Jan. 1972, pp. 343-353.

[19]Bamford, R. M., "A Modal Combination Program for Dynamic Analysis of Structures," Jet Propulsion Lab., Pasadena, CA, TM-33-290, July 1967.